

Search for pair production of second generation scalar leptoquarks in $p\bar{p}$ collisions at $\sqrt{s} = 1.96$ TeV

DØ Collaboration

V.M. Abazov^{an}, B. Abbott^{cc}, M. Abolins^{bs}, B.S. Acharya^{ag}, M. Adams^{bf}, T. Adams^{bd}, M. Agelou^u, J.-L. Agram^{v,w}, S.H. Ahn^{ai}, M. Ahsan^{bm}, G.D. Alexeev^{an}, G. Alkhazov^{ar}, A. Alton^{br}, G. Alverson^{bq}, G.A. Alves^b, M. Anastasoae^{am}, T. Andeen^{bh}, S. Anderson^{az}, B. Andrieu^t, M.S. Anzelc^{bh}, Y. Arnoud^q, M. Arov^{bg}, A. Askew^{bd}, B. Åsman^{as,at,au}, A.C.S. Assis Jesus^c, O. Atramentov^{bk}, C. Autermann^y, C. Avila^k, C. Ay^{ab}, F. Badaud^p, A. Baden^{bo}, L. Bagby^{bg}, B. Baldin^{be}, D.V. Bandurin^{an}, P. Banerjee^{ag}, S. Banerjee^{ag}, E. Barberis^{bq}, P. Bargassa^{ch}, P. Baringer^{bl}, C. Barnes^{ax}, J. Barreto^b, J.F. Bartlett^{be}, U. Bassler^t, D. Bauer^{bi}, A. Bean^{bl}, M. Begalli^c, M. Begel^{by}, A. Bellavance^{bu}, J. Benitez^{bs}, S.B. Beri^{ae}, G. Bernardi^t, R. Bernhard^{av}, L. Berntzon^r, I. Bertram^{aw}, M. Besançon^u, R. Beuselinck^{ax}, V.A. Bezzubov^{aq}, P.C. Bhat^{be}, V. Bhatnagar^{ae}, M. Binder^{ac}, C. Biscarat^{aw}, K.M. Black^{bp}, I. Blackler^{ax}, G. Blazey^{bg}, F. Blekman^{ax}, S. Blessing^{bd}, D. Bloch^{v,w}, U. Blumenschein^{aa}, A. Boehnlein^{be}, O. Boeriu^{bj}, T.A. Bolton^{bm}, F. Borchering^{be}, G. Borissov^{aw}, K. Bos^{al}, T. Bose^{bx}, A. Brandt^{cf}, R. Brock^{bs}, G. Brooijmans^{bx}, A. Bross^{be}, D. Brown^{cf}, N.J. Buchanan^{bd}, D. Buchholz^{bh}, M. Buehler^{ci}, V. Buescher^{aa}, S. Burdin^{be}, S. Burke^{az}, T.H. Burnett^{cj}, E. Busato^t, C.P. Buszello^{ax}, J.M. Butler^{bp}, S. Calvet^r, J. Cammin^{by}, S. Caron^{al}, W. Carvalho^c, B.C.K. Casey^{ce}, N.M. Cason^{bj}, H. Castilla-Valdez^{ak}, S. Chakrabarti^{ag}, D. Chakraborty^{bg}, K.M. Chan^{by}, A. Chandra^{ag}, D. Chapin^{ce}, F. Charles^{v,w}, E. Cheu^{az}, F. Chevallier^q, D.K. Cho^{bp}, S. Choi^{aj}, B. Choudhary^{af}, T. Christiansen^{ac,*}, L. Christofek^{bl}, D. Claes^{bu}, B. Clément^{v,w}, C. Clément^{as,at,au}, Y. Coadou^{e,f,g,h}, M. Cooke^{ch}, W.E. Cooper^{be}, D. Coppage^{bl}, M. Corcoran^{ch}, M.-C. Cousinou^r, B. Cox^{ay}, S. Crépe-Renaudin^q, D. Cutts^{ce}, M. Cwiok^{ah}, H. da Motta^b, A. Das^{bp}, M. Das^{bn}, B. Davies^{aw}, G. Davies^{ax}, G.A. Davis^{bh}, K. De^{cf}, P. de Jong^{al}, S.J. de Jong^{am}, E. De La Cruz-Burelo^{br}, C. De Oliveira Martins^c, J.D. Degenhardt^{br}, F. Déliot^u, M. Demarteau^{be}, R. Demina^{by}, P. Demine^u, D. Denisov^{be}, S.P. Denisov^{aq}, S. Desai^{bz}, H.T. Diehl^{be}, M. Diesburg^{be}, M. Doidge^{aw}, H. Dong^{bz}, S. Doulas^{bq}, L.V. Dudko^{ap}, L. Duflot^s, S.R. Dugad^{ag}, A. Duperrin^r, J. Dyer^{bs}, A. Dyshkant^{bg}, M. Eads^{bu}, D. Edmunds^{bs}, T. Edwards^{ay}, J. Ellison^{bc}, J. Elmsheuser^{ac}, V.D. Elvira^{be}, S. Eno^{bo}, P. Ermolov^{ap}, J. Estrada^{be}, H. Evans^{bi}, A. Evdokimov^{ao}, V.N. Evdokimov^{aq}, S.N. Fatakia^{bp}, L. Feligioni^{bp}, A.V. Ferapontov^{aq}, T. Ferbel^{by}, F. Fiedler^{ac}, F. Filthaut^{am}, W. Fisher^{be}, H.E. Fisk^{be}, I. Fleck^{aa}, M. Ford^{ay}, M. Fortner^{bg}, H. Fox^{aa}, S. Fu^{be}, S. Fuess^{be}, T. Gadfort^{cj}, C.F. Galea^{am}, E. Gallas^{be}, E. Galyaev^{bj}, C. Garcia^{by}, A. Garcia-Bellido^{cj}, J. Gardner^{bl}, V. Gavrilov^{ao}, A. Gay^{v,w}, P. Gay^p, D. Gelé^{v,w}, R. Gelhaus^{bc}, C.E. Gerber^{bf}, Y. Gershtein^{bd}, D. Gillberg^{e,f,g,h}, G. Ginther^{by}, T. Golling^z, N. Gollub^{as,at,au}, B. Gómez^k, K. Gounder^{be}, A. Goussiou^{bj}, P.D. Grannis^{bz}, S. Greder^c, H. Greenlee^{be}, Z.D. Greenwood^{bn}, E.M. Gregores^d, G. Grenier^x, Ph. Gris^p, J.-F. Grivaz^s, S. Grünendahl^{be}, M.W. Grünewald^{ah}, J. Guo^{bz}, G. Gutierrez^{be}, P. Gutierrez^{cc}, A. Haas^{bx}, N.J. Hadley^{bo}, P. Haefner^{ac},

S. Hagopian^{bd}, J. Haley^{bv}, I. Hall^{cc}, R.E. Hall^{bb}, L. Han^j, K. Hanagaki^{be}, K. Harder^{bm}, A. Harel^{by}, R. Harrington^{bq}, J.M. Hauptman^{bk}, R. Hauser^{bs}, J. Hays^{bh}, T. Hebbeker^y, D. Hedin^{bg}, J.G. Hegeman^{al}, J.M. Heinmiller^{bf}, A.P. Heinson^{bc}, U. Heintz^{bp}, C. Hensel^{bl}, G. Hesketh^{bq}, M.D. Hildreth^{bj}, R. Hirosky^{ci}, J.D. Hobbs^{bz}, B. Hoeneisen^o, M. Hohlfeld^s, S.J. Hong^{ai}, R. Hooper^{ce}, P. Houben^{al}, Y. Hu^{bz}, V. Hynek^l, I. Iashvili^{bw}, R. Illingworth^{be}, A.S. Ito^{be}, S. Jabeen^{bl}, M. Jaffré^s, S. Jain^{cc}, K. Jakobs^{aa}, C. Jarvis^{bo}, A. Jenkins^{ax}, R. Jesik^{ax}, K. Johns^{az}, C. Johnson^{bx}, M. Johnson^{be}, A. Jonckheere^{be}, P. Jonsson^{ax}, A. Juste^{be}, D. Käfer^y, S. Kahn^{ca}, E. Kajfasz^r, A.M. Kalinin^{an}, J.M. Kalk^{bn}, J.R. Kalk^{bs}, D. Karmanov^{ap}, J. Kasper^{bp}, I. Katsanos^{bx}, D. Kau^{bd}, R. Kaur^{ae}, R. Kehoe^{cg}, S. Kermiche^r, S. Kesisoglou^{ce}, A. Khanov^{cd}, A. Kharchilava^{bw}, Y.M. Kharzheev^{an}, D. Khatidze^{bx}, H. Kim^{cf}, T.J. Kim^{ai}, M.H. Kirby^{am}, B. Klima^{be}, J.M. Kohli^{ae}, J.-P. Konrath^{aa}, M. Kopal^{cc}, V.M. Korablev^{aq}, J. Kotcher^{ca}, B. Kothari^{bx}, A. Koubarovsky^{ap}, A.V. Kozelov^{aq}, J. Kozminski^{bs}, A. Kryemadhi^{ci}, S. Krzywdzinski^{be}, T. Kuhl^{ab}, A. Kumar^{bw}, S. Kunori^{bo}, A. Kupcoⁿ, T. Kurča^{x,l}, J. Kvita^l, S. Lager^{as,at,au}, S. Lammers^{bx}, G. Landsberg^{ce}, J. Lazoflores^{bd}, A.-C. Le Bihan^{v,w}, P. Lebrun^x, W.M. Lee^{bg}, A. Leflat^{ap}, F. Lehner^{av}, C. Leonidopoulos^{bx}, V. Lesne^p, J. Leveque^{az}, P. Lewis^{ax}, J. Li^{cf}, Q.Z. Li^{be}, J.G.R. Lima^{bg}, D. Lincoln^{be}, J. Linnemann^{bs}, V.V. Lipaev^{aq}, R. Lipton^{be}, L. Lobo^{ax}, A. Lobodenko^{ar}, M. Lokajicekⁿ, A. Lounis^{v,w}, P. Love^{aw}, H.J. Lubatti^{cj}, M. Lynker^{bj}, A.L. Lyon^{be}, A.K.A. Maciel^b, R.J. Madaras^{ba}, P. Mättig^{ad}, C. Magass^y, A. Magerkurth^{br}, A.-M. Magnan^q, N. Makovec^s, P.K. Mal^{bj}, H.B. Malbouisson^c, S. Malik^{bu}, V.L. Malyshev^{an}, H.S. Maoⁱ, Y. Maravin^{bm}, M. Martens^{be}, S.E.K. Mattingly^{ce}, R. McCarthy^{bz}, R. McCroskey^{az}, D. Meder^{ab}, A. Melnitchouk^{bt}, A. Mendes^r, L. Mendoza^k, M. Merkin^{ap}, K.W. Merritt^{be}, A. Meyer^y, J. Meyer^z, M. Michaut^u, H. Miettinen^{ch}, J. Mitrevski^{bx}, J. Molina^c, N.K. Mondal^{ag}, J. Monk^{ay}, R.W. Moore^{e,f,g,h}, T. Moulik^{bl}, G.S. Muanza^s, M. Mulders^{be}, L. Mundim^c, Y.D. Mutaf^{bz}, E. Nagy^r, M. Naimuddin^{af}, M. Narain^{bp}, N.A. Naumann^{am}, H.A. Neal^{br}, J.P. Negret^k, S. Nelson^{bd}, P. Neustroev^{ar}, C. Noeding^{aa}, A. Nomerotski^{be}, S.F. Novaes^d, T. Nunnemann^{ac}, E. Nurse^{ay}, V. O'Dell^{be}, D.C. O'Neil^{e,f,g,h}, G. Obrant^{ar}, V. Oguri^c, N. Oliveira^c, N. Oshima^{be}, R. Otec^m, G.J. Otero y Garzón^{bf}, M. Owen^{ay}, P. Padley^{ch}, N. Parashar^{be,2}, S.K. Park^{ai}, J. Parsons^{bx}, R. Partridge^{ce}, N. Parua^{bz}, A. Patwa^{ca}, G. Pawloski^{ch}, P.M. Perea^{bc}, E. Perez^u, P. Pétrouff^s, M. Petteni^{ax}, R. Piegaia^a, M.-A. Pleier^z, P.L.M. Podesta-Lerma^{ak}, V.M. Podstavkov^{be}, Y. Pogorelov^{bj}, M.-E. Pol^b, A. Pompoš^{cc}, B.G. Pope^{bs}, A.V. Popov^{aq}, W.L. Prado da Silva^c, H.B. Prosper^{bd}, S. Protopopescu^{ca}, J. Qian^{br}, A. Quadt^z, B. Quinn^{bt}, K.J. Rani^{ag}, K. Ranjan^{af}, P.A. Rapidis^{be}, P.N. Ratoff^{aw}, P. Renkel^{cg}, S. Reucroft^{bq}, M. Rijssenbeek^{bz}, I. Ripp-Baudot^{v,w}, F. Rizatdinova^{cd}, S. Robinson^{ax}, R.F. Rodrigues^c, C. Royon^u, P. Rubinov^{be}, R. Ruchti^{bj}, V.I. Rud^{ap}, G. Sajot^q, A. Sánchez-Hernández^{ak}, M.P. Sanders^{bo}, A. Santoro^c, G. Savage^{be}, L. Sawyer^{bn}, T. Scanlon^{ax}, D. Schaile^{ac}, R.D. Schamberger^{bz}, Y. Scheglov^{ar}, H. Schellman^{bh}, P. Schieferdecker^{ac}, C. Schmitt^{ad}, C. Schwanenberger^z, A. Schwartzman^{bv}, R. Schwienhorst^{bs}, S. Sengupta^{bd}, H. Severini^{cc}, E. Shabalina^{bf}, M. Shamim^{bm}, V. Shary^u, A.A. Shchukin^{aq}, W.D. Shephard^{bj}, R.K. Shivpuri^{af}, D. Shpakov^{bq}, V. Siccaldi^{v,w}, R.A. Sidwell^{bm}, V. Simak^m, V. Sirotenko^{be}, P. Skubic^{cc}, P. Slattery^{by}, R.P. Smith^{be}, G.R. Snow^{bu}, J. Snow^{cb}, S. Snyder^{ca}, S. Söldner-Rembold^{ay}, X. Song^{bg}, L. Sonnenschein^t, A. Sopczak^{aw}, M. Sosebee^{cf}, K. Soustruznik^l, M. Souza^b, B. Spurlock^{cf}, J. Stark^q, J. Steele^{bn}, K. Stevenson^{bi}, V. Stolin^{ao}, A. Stone^{bf}, D.A. Stoyanova^{aq}, J. Strandberg^{as,at,au}, M.A. Strang^{bw}, M. Strauss^{cc}, R. Ströhmer^{ac}, D. Strom^{bh}, M. Strovink^{ba}, L. Stutte^{be}, S. Sumowidagdo^{bd}, A. Sznajder^c, M. Talby^r, P. Tamburello^{az}, W. Taylor^{e,f,g,h}, P. Telford^{ay}, J. Temple^{az}, B. Tiller^{ac}, M. Titov^{aa}, V.V. Tokmenin^{an}, M. Tomoto^{be}, T. Toole^{bo}, I. Torchiani^{aa}, S. Towers^{aw}, T. Trefzger^{ab}, S. Trincaz-Duvoid^t, D. Tsybychev^{bz},

B. Tuchming^u, C. Tully^{bv}, A.S. Turcot^{ay}, P.M. Tuts^{bx}, R. Unalan^{bs}, L. Uvarov^{ar}, S. Uvarov^{ar}, S. Uzunyan^{bg}, B. Vachon^{e,f,g,h}, P.J. van den Berg^{al}, R. Van Kooten^{bi}, W.M. van Leeuwen^{al}, N. Varelas^{bf}, E.W. Varnes^{az}, A. Vartapetian^{cf}, I.A. Vasilyev^{aq}, M. Vaupel^{ad}, P. Verdier^x, L.S. Vertogradov^{an}, M. Verzocchi^{be}, F. Villeneuve-Seguier^{ax}, J.-R. Vlimant^t, E. Von Toerne^{bm}, M. Voutilainen^{bu,3}, M. Vreeswijk^{al}, H.D. Wahl^{bd}, L. Wang^{bo}, J. Warchol^{bj}, G. Watts^{cj}, M. Wayne^{bj}, M. Weber^{be}, H. Weerts^{bs}, N. Vermes^z, M. Wetstein^{bo}, A. White^{cf}, V. White^{be}, D. Wicke^{ad}, D.A. Wijngaarden^{am}, G.W. Wilson^{bl}, S.J. Wimpenny^{bc}, M. Wobisch^{be}, J. Womersley^{be}, D.R. Wood^{bq}, T.R. Wyatt^{ay}, Y. Xie^{ce}, N. Xuan^{bj}, S. Yacoob^{bh}, R. Yamada^{be}, M. Yan^{bo}, T. Yasuda^{be}, Y.A. Yatsunenko^{an}, Y. Yen^{ad}, K. Yip^{ca}, H.D. Yoo^{ce}, S.W. Youn^{bh}, J. Yu^{cf}, A. Yurkewicz^{bz}, A. Zatserklyaniy^{bg}, C. Zeitnitz^{ad}, D. Zhang^{be}, T. Zhao^{cj}, Z. Zhao^{br}, B. Zhou^{br}, J. Zhu^{bz}, M. Zielinski^{by}, D. Zieminska^{bi}, A. Zieminski^{bi}, V. Zutshi^{bg}, E.G. Zverev^{ap}

^a Universidad de Buenos Aires, Buenos Aires, Argentina

^b LAFEX, Centro Brasileiro de Pesquisas Físicas, Rio de Janeiro, Brazil

^c Universidade do Estado do Rio de Janeiro, Rio de Janeiro, Brazil

^d Instituto de Física Teórica, Universidade Estadual Paulista, São Paulo, Brazil

^e University of Alberta, Edmonton, AB, Canada

^f Simon Fraser University, Burnaby, BC, Canada

^g York University, Toronto, ON, Canada

^h McGill University, Montreal, PQ, Canada

ⁱ Institute of High Energy Physics, Beijing, People's Republic of China

^j University of Science and Technology of China, Hefei, People's Republic of China

^k Universidad de los Andes, Bogotá, Colombia

^l Center for Particle Physics, Charles University, Prague, Czech Republic

^m Czech Technical University, Prague, Czech Republic

ⁿ Center for Particle Physics, Institute of Physics, Academy of Sciences of the Czech Republic, Prague, Czech Republic

^o Universidad San Francisco de Quito, Quito, Ecuador

^p Laboratoire de Physique Corpusculaire, IN2P3-CNRS, Université Blaise Pascal, Clermont-Ferrand, France

^q Laboratoire de Physique Subatomique et de Cosmologie, IN2P3-CNRS, Université de Grenoble 1, Grenoble, France

^r CPPM, IN2P3-CNRS, Université de la Méditerranée, Marseille, France

^s IN2P3-CNRS, Laboratoire de l'Accélérateur Linéaire, Orsay, France

^t LPNHE, IN2P3-CNRS, Universités Paris VI and VII, Paris, France

^u DAPNIA/Service de Physique des Particules, CEA, Saclay, France

^v IReS, IN2P3-CNRS, Université Louis Pasteur, Strasbourg, France

^w Université de Haute Alsace, Mulhouse, France

^x Institut de Physique Nucléaire de Lyon, IN2P3-CNRS, Université Claude Bernard, Villeurbanne, France

^y III. Physikalisches Institut A, RWTH Aachen, Aachen, Germany

^z Physikalisches Institut, Universität Bonn, Bonn, Germany

^{aa} Physikalisches Institut, Universität Freiburg, Freiburg, Germany

^{ab} Institut für Physik, Universität Mainz, Mainz, Germany

^{ac} Ludwig-Maximilians-Universität München, München, Germany

^{ad} Fachbereich Physik, University of Wuppertal, Wuppertal, Germany

^{ae} Panjab University, Chandigarh, India

^{af} Delhi University, Delhi, India

^{ag} Tata Institute of Fundamental Research, Mumbai, India

^{ah} University College Dublin, Dublin, Ireland

^{ai} Korea Detector Laboratory, Korea University, Seoul, South Korea

^{aj} SungKyunKwan University, Suwon, South Korea

^{ak} CINVESTAV, Mexico City, Mexico

^{al} FOM-Institute NIKHEF and University of Amsterdam/NIKHEF, Amsterdam, The Netherlands

^{am} Radboud University Nijmegen/NIKHEF, Nijmegen, The Netherlands

^{an} Joint Institute for Nuclear Research, Dubna, Russia

^{ao} Institute for Theoretical and Experimental Physics, Moscow, Russia

^{ap} Moscow State University, Moscow, Russia

^{aq} Institute for High Energy Physics, Protvino, Russia

^{ar} Petersburg Nuclear Physics Institute, St. Petersburg, Russia

^{as} Lund University, Lund, Sweden

^{at} Royal Institute of Technology and Stockholm University, Stockholm, Sweden

^{au} Uppsala University, Uppsala, Sweden

^{av} Physik Institut der Universität Zürich, Zürich, Switzerland

^{aw} Lancaster University, Lancaster, United Kingdom

^{ax} Imperial College, London, United Kingdom

^{ay} University of Manchester, Manchester, United Kingdom

^{az} University of Arizona, Tucson, AZ 85721, USA

^{ba} Lawrence Berkeley National Laboratory and University of California, Berkeley, CA 94720, USA

^{bb} California State University, Fresno, CA 93740, USA

^{bc} University of California, Riverside, CA 92521, USA

^{bd} Florida State University, Tallahassee, FL 32306, USA

^{be} Fermi National Accelerator Laboratory, Batavia, IL 60510, USA

^{bf} University of Illinois at Chicago, Chicago, IL 60607, USA

^{bg} Northern Illinois University, DeKalb, IL 60115, USA

^{bh} Northwestern University, Evanston, IL 60208, USA

^{bi} Indiana University, Bloomington, IN 47405, USA

^{bj} University of Notre Dame, Notre Dame, IN 46556, USA

^{bk} Iowa State University, Ames, IA 50011, USA

^{bl} University of Kansas, Lawrence, KS 66045, USA

^{bm} Kansas State University, Manhattan, KS 66506, USA

^{bn} Louisiana Tech University, Ruston, LA 71272, USA

^{bo} University of Maryland, College Park, MD 20742, USA

^{bp} Boston University, Boston, MA 02215, USA

^{bq} Northeastern University, Boston, MA 02115, USA

^{br} University of Michigan, Ann Arbor, MI 48109, USA

^{bs} Michigan State University, East Lansing, MI 48824, USA

^{bt} University of Mississippi, University, MI 38677, USA

^{bu} University of Nebraska, Lincoln, NB 68588, USA

^{bv} Princeton University, Princeton, NJ 08544, USA

^{bw} State University of New York, Buffalo, NY 14260, USA

^{bx} Columbia University, New York, NY 10027, USA

^{by} University of Rochester, Rochester, NY 14627, USA

^{bz} State University of New York, Stony Brook, NY 11794, USA

^{ca} Brookhaven National Laboratory, Upton, NY 11973, USA

^{cb} Langston University, Langston, OK 73050, USA

^{cc} University of Oklahoma, Norman, OK 73019, USA

^{cd} Oklahoma State University, Stillwater, OK 74078, USA

^{ce} Brown University, Providence, RI 02912, USA

^{cf} University of Texas, Arlington, TX 76019, USA

^{cg} Southern Methodist University, Dallas, TX 75275, USA

^{ch} Rice University, Houston, TX 77005, USA

^{ci} University of Virginia, Charlottesville, VI 22901, USA

^{cj} University of Washington, Seattle, WA 98195, USA

Received 31 January 2006; received in revised form 23 March 2006; accepted 29 March 2006

Available online 7 April 2006

Editor: L. Rolandi

Abstract

We report on a search for the pair production of second generation scalar leptoquarks (LQ_2) in $p\bar{p}$ collisions at the center-of-mass energy $\sqrt{s} = 1.96$ TeV, using data corresponding to an integrated luminosity of 294 ± 19 pb $^{-1}$ recorded with the DØ detector. No evidence for a leptoquark signal in the $LQ_2\bar{LQ}_2 \rightarrow \mu q\mu q$ channel has been observed, and upper bounds on the product of cross section times branching fraction were set. This yields lower mass limits of $m_{LQ_2} > 247$ GeV/ c^2 for $\beta = \mathcal{B}(LQ_2 \rightarrow \mu q) = 1$ and $m_{LQ_2} > 182$ GeV/ c^2 for $\beta = 1/2$. Combining these limits with previous DØ results, the lower limits on the mass of a second generation scalar leptoquark are $m_{LQ_2} > 251$ GeV/ c^2 and $m_{LQ_2} > 204$ GeV/ c^2 for $\beta = 1$ and $\beta = 1/2$, respectively.

© 2006 Elsevier B.V. All rights reserved.

PACS: 14.80.-j; 13.85.Rm

Keywords: Second generation leptoquarks

* Corresponding author.

E-mail address: tim.christiansen@cern.ch (T. Christiansen).

¹ On leave from IEP SAS Kosice, Slovakia.

² Visitor from Purdue University Calumet, Hammond, IN, USA.

³ Visitor from Helsinki Institute of Physics, Helsinki, Finland.

Leptoquarks, colored bosons which carry both lepton (l) and quark (q) quantum numbers and an electric charge that is an integer multiple of $e/3$, appear in several extensions of the standard model of particle physics [1]. Leptoquarks could, in principle, decay into any combination of a lepton and a quark.

Experimental limits on lepton number violation, on flavor-changing neutral currents, and on proton decay, however, motivate the assumption that there would be three different generations of leptoquarks. Each of these leptoquark generations couples to only one generation of quarks and leptons, and, therefore, conserves the corresponding lepton and quark family numbers [2]. As a consequence, leptoquark masses could be as low as $\mathcal{O}(100 \text{ GeV}/c^2)$, allowing the production of leptoquarks in reach of present collider experiments.

At the Tevatron collider, scalar leptoquarks would be produced in pairs, primarily through $q\bar{q}$ annihilation and gluon fusion. These production mechanisms would be independent of the unknown coupling λ between the leptoquark, the lepton, and the quark.

This analysis focuses on the search for pair-produced second generation scalar leptoquarks (LQ_2) in $p\bar{p}$ collisions at $\sqrt{s} = 1.96 \text{ TeV}$. Assuming 100% branching fraction to a charged lepton and a quark, $\beta = \mathcal{B}(LQ_2 \rightarrow \mu q) = 1$, a pair of second generation leptoquarks, $LQ_2\bar{LQ}_2$, decays into two muons and two quarks. This decay will have no missing transverse energy. For $\beta = 1/2$, the same final state is produced 25% of the time. The DØ Collaboration published 95% confidence level (C.L.) mass limits for second generation scalar leptoquarks of $m_{LQ_2} > 200 \text{ GeV}/c^2$ ($180 \text{ GeV}/c^2$) for $\beta = 1$ ($1/2$) at $\sqrt{s} = 1.8 \text{ TeV}$, using 94 pb^{-1} of Run I Tevatron data [3]. Recent CDF analyses of dimuon + jet and single muon + jet Run II Tevatron data give $m_{LQ_2} > 226 \text{ GeV}/c^2$ ($208 \text{ GeV}/c^2$) for $\beta = 1$ ($1/2$), determined from 198 pb^{-1} of data [4].

The DØ Run II detector [5] is composed of several layered elements. Nearest the beam is a central tracking system consisting of a silicon microstrip tracker (SMT) and a central fiber tracker (CFT), both located within a 2 T superconducting solenoidal magnet. Muon momenta are measured from the curvature of muon tracks in the central tracking system. Jets are reconstructed from energy depositions in the three liquid-argon/uranium calorimeters outside the tracking system: a central section (CC) covering up to $|\eta| \approx 1.1$ and two end calorimeters (EC) extending coverage to $|\eta| \approx 4$, all housed in separate cryostats, where $\eta = -\ln(\tan \frac{\theta}{2})$ denotes the pseudorapidity and θ is the polar angle with respect to the proton beam direction. Scintillators located between the CC and EC cryostats provide sampling of hadron showers for $1.1 < |\eta| < 1.4$. A muon system beyond the calorimeters consists of a layer of drift-tube tracking detectors and scintillation trigger counters before 1.8 T iron toroids, followed by two additional similar layers after the toroids [6].

The data used in this analysis were collected during Run II of the Fermilab Tevatron collider between August 2002 and July 2004 and correspond to an integrated luminosity of $294 \pm 19 \text{ pb}^{-1}$. The sample of candidate events used in this search was collected with a set of triggers that required either one or two muon candidates in the muon system. The trigger efficiency for the $\mu_j\mu_j$ events considered in this analysis was measured to be $(89 \pm 3)\%$.

Muons in the region $|\eta| < 1.9$ were reconstructed offline from hits in the three layers of the muon system which were

matched to isolated tracks in the central tracking system to remove the background from heavy-quark production. This muon isolation was assured by requiring the sum of the transverse momenta of all other tracks (with transverse momentum $p_T > 180 \text{ MeV}/c$) in a $\Delta\mathcal{R} = \sqrt{(\Delta\phi)^2 + (\Delta\eta)^2} < 0.5$ cone around the muon to be smaller than $4 \text{ GeV}/c$, where ϕ is the azimuthal angle around the direction of the incident beam. Cosmic ray muons were rejected by cuts on the timing in the muon scintillators and by removing back-to-back muons. Jets were reconstructed using the iterative, midpoint cone algorithm [7] with a cone size of $\Delta\mathcal{R} = 0.5$. The jet energies were calibrated as a function of the jet transverse energy and η by balancing the transverse energy in photon plus jet events. Requiring $|\eta| < 2.4$ for all jets removes the QCD background from events with jets at very small angles to the beam direction and, therefore, with large cross sections.

The background is dominated by the Drell–Yan (DY) events in the channel $Z/\gamma^* \rightarrow \mu\mu$ (+jets). QCD multijet events faking muons are suppressed by the isolation requirement and the thick shielding of the muon detectors. To evaluate the contribution from DY background, samples of Monte Carlo (MC) events were generated with PYTHIA [8]. The number of PYTHIA events was normalized to yield the predicted next-to-next-to-leading order (NNLO) cross section [9] at the Z -boson resonance. The events were furthermore reweighted as a function of the dimuon mass in order to describe the NNLO prediction for the differential cross section $d\sigma/dm(\mu\mu)$ [9]. An additional sample, generated with ALPGEN [10] and based on a matrix-element calculation for Zjj , was used to test systematic uncertainties due to the shape of the jet transverse energy distribution. Samples of PYTHIA $t\bar{t}$ ($m_t = 175 \text{ GeV}/c^2$) and WW samples were used to estimate the background contributions from top quark and W boson pair production. The signal efficiencies were calculated using samples of $LQ_2\bar{LQ}_2 \rightarrow \mu q\mu q$ events simulated with PYTHIA for leptoquark masses from 140 to $300 \text{ GeV}/c^2$ in steps of $20 \text{ GeV}/c^2$. All Monte Carlo events were generated using CTEQ5L [11] parton distribution functions (PDFs) and processed using a full simulation of the DØ detector based on GEANT [12] and the DØ event reconstruction [5].

Offline, events were required to have two muons with transverse momenta p_T exceeding $15 \text{ GeV}/c$ and at least two jets with transverse energies E_T greater than 25 GeV . The momentum resolution degrades with increasing p_T , and hence the resolution on the dimuon mass $m(\mu\mu)$ with increasing $m(\mu\mu)$. Therefore, in order to reduce the DY background at high $m(\mu\mu)$ and to account for muon tracks with large momentum uncertainty, corrections were applied to the muon momenta by taking advantage of the fact that no missing transverse energy is expected in either signal or DY events. The missing transverse energy \cancel{E}_T was estimated from the transverse energy balance of all muons and jets ($E_T > 20 \text{ GeV}$) in the event. The momentum of the muon most opposite to the \cancel{E}_T direction in the r - ϕ plane (i.e., in the plane perpendicular to the incident beam) was rescaled such that the component of the missing transverse energy parallel to the muon vanished. This correction suppressed the contribution from Z boson events misreconstructed in the high mass region where the search for leptoquarks took place.

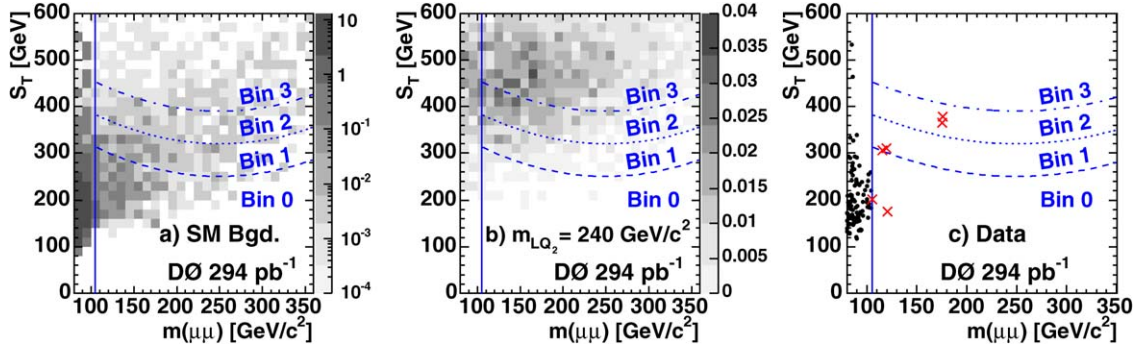


Fig. 1. Scalar sum of the transverse energies, S_T , as a function of the dimuon mass: (a) for the SM background, (b) for leptoquark signal with mass $m_{LQ_2} = 240 \text{ GeV}/c^2$ and $\beta = 1$, and (c) for data (the six events surviving the Z boson veto are highlighted). The vertical line illustrates the Z boson veto and the curved lines show the boundaries between the signal bins (see text for definition). The distributions shown in (a) and (b) are normalized to the integrated luminosity.

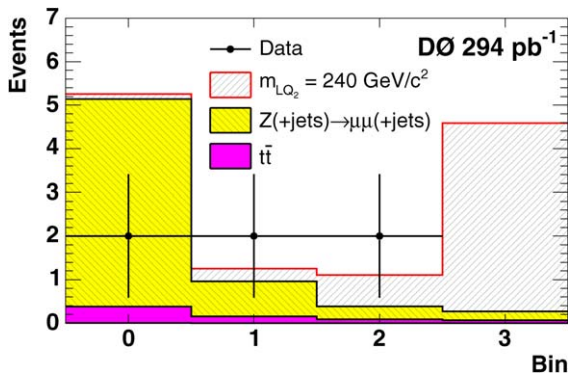


Fig. 2. Distribution of events over the four bins as defined in the text for a scalar leptoquark with mass $m_{LQ_2} = 240 \text{ GeV}/c^2$ and $\beta = 1$.

To further reduce the background from DY events a Z boson veto cut (dimuon mass $m(\mu\mu) > 105 \text{ GeV}/c^2$) was applied. Six events survive this last cut, while 6.8 ± 2.0 events are expected from standard model backgrounds, which mainly consists of DY (6.1 ± 2.0) and $t\bar{t}$ (0.69 ± 0.07).

The remaining events after the Z boson veto cut were arranged in four bins. Second generation leptoquark events are expected to have both high dimuon masses and large values of S_T , which is the scalar sum of the transverse energies of the two highest- p_T muons and the two highest- E_T jets in the event, as can be seen in Fig. 1(b) for a leptoquark mass of $240 \text{ GeV}/c^2$. The separation between bin i and bin $i - 1$, $i \in \{1, 2, 3\}$, is defined as

$$S_T > \frac{0.003c^4}{\text{GeV}} (m(\mu\mu) - 250 \text{ GeV}/c^2)^2 + 180 \text{ GeV} + i \cdot 70 \text{ GeV}.$$

This binning, which effectively results in bins in the order of increasing S/B , is illustrated by the curved lines in Fig. 1 for the expected standard model backgrounds, an example LQ_2 signal, and for the data. The number of events in the four signal bins is shown in Fig. 2.

Table 1 summarizes the efficiencies for various leptoquark masses, as well as the numbers of expected background events and the distribution of the data in the four signal bins. The signal efficiency increases with mass, because for larger lepto-

quark masses, the decay products have larger momenta yielding events with larger S_T . The dominant uncertainty on the predicted number of background events is due to MC statistics and varies between 7% and 25% for the four signal bins. Other contributions arise from the jet-energy calibration uncertainty (2%–12%) and the uncertainty in the shape of the jet transverse energy distribution (20%), which has been estimated by a comparison of the PYTHIA and ALPGEN simulations. The jet multiplicity in DY events generated with PYTHIA, which is a leading-order generator, was corrected in order to reflect the multiplicity distribution observed in the data around the Z boson. This was accomplished by comparing exponential fits to the inclusive jet multiplicity distribution in data and Monte Carlo. The fit is dominated by the zero and one jet bins. The remaining difference in the two jet bin between $\mu j \mu j$ events in data and in the PYTHIA Monte Carlo in the vicinity of the Z boson resonance, $60 \text{ GeV}/c^2 < m(\mu\mu) < 105 \text{ GeV}/c^2$, was taken as the corresponding systematic uncertainty (16%). In addition, the following sources of systematic uncertainties were taken into account: luminosity (6.5%), PDF uncertainty of the DY processes (3.6%), and muon triggering and identification (5%). The systematics, added in quadrature, are shown in Table 1. The systematic uncertainties on the signal efficiencies arise from limited Monte Carlo statistics (2%–17%), jet-energy scale (3%–13%), muon triggering and identification (5%), and PDF uncertainty (2%).

No significant excess of data over background was observed. Upper limits on the product of cross section times branching fraction, $\sigma \cdot \beta^2$, were calculated as described in Ref. [13], by treating the four signal bins as individual channels. The likelihoods for the different bins were combined with correlations of systematic uncertainties taken into account. The limits are calculated using the confidence level $CL_S = CL_{S+B}/CL_B$, where CL_{S+B} is the confidence level for the signal plus background hypothesis and CL_B is the confidence level for the background only [13].

The limits on the cross section times branching fraction and the theoretical predictions [14] are shown in Fig. 3 and Table 2, as well as the average expected limit assuming that no signal is present. Due to the larger background, the contribution of bin 0 to the limit is relatively small. This explains why the average ex-

Table 1

Signal efficiency (ε) for various scalar leptoquark masses, number of expected background events ($N_{\text{pred}}^{\text{bgd}}$), and the number of data events (N_{data})

| Cut | $m(\mu\mu) > 105 \text{ GeV}/c^2$ | Bin 0 | Bin 1 | Bin 2 | Bin 3 |
|------------------------------------|-----------------------------------|-------------------|-------------------|-------------------|-------------------|
| $\varepsilon(140 \text{ GeV}/c^2)$ | 0.139 ± 0.013 | 0.041 ± 0.004 | 0.036 ± 0.004 | 0.025 ± 0.003 | 0.038 ± 0.005 |
| $\varepsilon(160 \text{ GeV}/c^2)$ | 0.174 ± 0.016 | 0.026 ± 0.004 | 0.042 ± 0.004 | 0.040 ± 0.005 | 0.067 ± 0.008 |
| $\varepsilon(180 \text{ GeV}/c^2)$ | 0.197 ± 0.018 | 0.017 ± 0.002 | 0.038 ± 0.004 | 0.049 ± 0.005 | 0.093 ± 0.011 |
| $\varepsilon(200 \text{ GeV}/c^2)$ | 0.215 ± 0.019 | 0.009 ± 0.002 | 0.026 ± 0.004 | 0.047 ± 0.005 | 0.133 ± 0.015 |
| $\varepsilon(220 \text{ GeV}/c^2)$ | 0.223 ± 0.020 | 0.005 ± 0.001 | 0.016 ± 0.003 | 0.039 ± 0.005 | 0.163 ± 0.017 |
| $\varepsilon(240 \text{ GeV}/c^2)$ | 0.243 ± 0.021 | 0.005 ± 0.001 | 0.013 ± 0.002 | 0.032 ± 0.004 | 0.193 ± 0.018 |
| $\varepsilon(260 \text{ GeV}/c^2)$ | 0.251 ± 0.022 | 0.004 ± 0.001 | 0.009 ± 0.002 | 0.025 ± 0.004 | 0.212 ± 0.019 |
| $\varepsilon(280 \text{ GeV}/c^2)$ | 0.256 ± 0.022 | 0.003 ± 0.001 | 0.006 ± 0.001 | 0.018 ± 0.003 | 0.229 ± 0.020 |
| $\varepsilon(300 \text{ GeV}/c^2)$ | 0.263 ± 0.023 | 0.004 ± 0.001 | 0.004 ± 0.001 | 0.013 ± 0.002 | 0.242 ± 0.021 |
| $N_{\text{pred}}^{\text{bgd}}$ | 6.760 ± 1.999 | 5.140 ± 1.565 | 0.958 ± 0.374 | 0.388 ± 0.144 | 0.274 ± 0.138 |
| N_{data} | 6 | 2 | 2 | 2 | 0 |

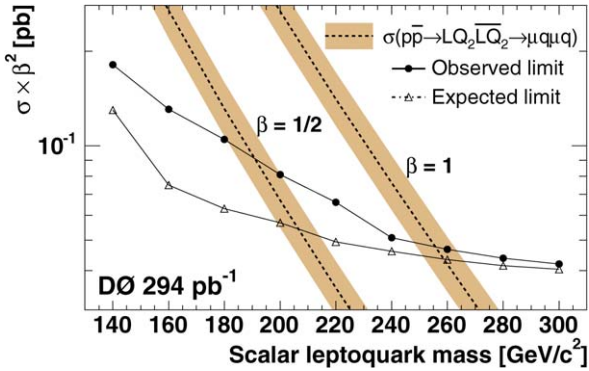


Fig. 3. Observed (closed circles) and expected (open triangles) 95% C.L. upper limit on production cross section times branching fraction for second generation scalar leptoquarks. The NLO theoretical predictions are also shown with error bands for $\beta = 1$ and $1/2$.

Table 2

NLO cross sections for scalar leptoquark pair production in $p\bar{p}$ collisions at $\sqrt{s} = 1.96 \text{ TeV}$, expected and observed 95% C.L. upper limits on the cross section times branching fraction for the analysis described in this Letter, and observed upper limits for the Run I + Run II combination. The cross sections shown are calculated using CTEQ6.1M as PDF [15] and m_{LQ_2} as the factorization/renormalization scale [14]. The uncertainties in the theoretical cross sections originate from a variation of the renormalization and factorization scale between $m_{LQ_2}/2$ and $2m_{LQ_2}$ and the PDF errors, added in quadrature

| m_{LQ_2} [GeV/ c^2] | $\sigma_{\text{theory}}^{\text{Run II}}$ [pb] $\sqrt{s} = 1.96 \text{ TeV}$ | Run II limits on $\sigma \cdot \beta^2$ [pb] | | Run I + II limits on $\sigma \cdot \beta^2$ [pb] |
|-----------------------------|--|--|------------|---|
| | | (expected) | (observed) | |
| 140 | $2.380^{+0.487}_{-0.448}$ | 0.130 | 0.181 | 0.144 |
| 160 | $1.080^{+0.225}_{-0.200}$ | 0.075 | 0.131 | 0.104 |
| 180 | $0.525^{+0.111}_{-0.096}$ | 0.063 | 0.105 | 0.083 |
| 200 | $0.268^{+0.057}_{-0.049}$ | 0.057 | 0.081 | 0.064 |
| 220 | $0.141^{+0.030}_{-0.025}$ | 0.049 | 0.066 | 0.052 |
| 240 | $0.076^{+0.017}_{-0.015}$ | 0.046 | 0.051 | 0.045 |
| 260 | $0.042^{+0.009}_{-0.008}$ | 0.043 | 0.047 | 0.042 |
| 280 | $0.023^{+0.005}_{-0.004}$ | 0.042 | 0.044 | 0.038 |
| 300 | $0.013^{+0.003}_{-0.002}$ | 0.040 | 0.042 | 0.037 |

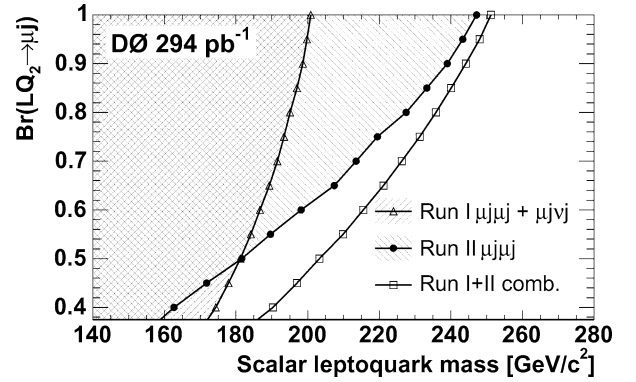


Fig. 4. In the (m_{LQ_2}, β) plane, regions excluded at 95% C.L. by the DØ Run I results, by this analysis, and by the combination of the two.

pected limit is better than the observed limit, although the sum of the events in all four bins is comparable to the background prediction. The mass limit is extracted from the intersection of the lower edge of the next-to-leading order (NLO) cross section uncertainty band with the observed upper bound on the cross section. The uncertainty band reflects the PDF uncertainty [15] as well as the variation of the factorization and renormalization scale between $m_{LQ_2}/2$ and $2m_{LQ_2}$, added in quadrature.

The lower limit on the mass of second generation scalar leptoquarks was determined at the 95% C.L. to be $m_{LQ_2} > 247 \text{ GeV}/c^2$ and $m_{LQ_2} > 182 \text{ GeV}/c^2$ for $\beta = 1$ and $\beta = 1/2$, respectively. The average expected limits are $m_{LQ_2}^{\text{expected}} > 251 \text{ GeV}/c^2$ and $m_{LQ_2}^{\text{expected}} > 199 \text{ GeV}/c^2$. Fig. 4 shows the excluded region in the β versus m_{LQ_2} parameter space.

The DØ Run I analysis in the $\mu j \mu j$ channel had no events after all cuts, while 0.7 ± 0.5 events were expected from the background. A complementary Run I analysis in the $\mu j \nu j$ channel yielded no events for 0.7 ± 0.9 events expected from standard model background [3]. Taking into account the smaller cross section for the production of second generation scalar leptoquarks at the Run I center-of-mass energy $\sqrt{s} = 1.8 \text{ TeV}$, these earlier results have been combined with the Run II analysis presented in this Letter. The combination was performed by treating the two results from Run I as additional bins to

the limit calculation. The results are summarized in Table 2 and the excluded parameter regions are shown in Fig. 4. The combined lower limit for scalar leptoquarks of the second generation is $m_{LQ_2} > 251 \text{ GeV}/c^2$ ($m_{LQ_2} > 204 \text{ GeV}/c^2$) for $\beta = 1$ ($\beta = 1/2$). These results improve on previous measurements at the Tevatron collider [3,4] and are, for large β , the most stringent limits on second generation scalar leptoquarks from direct measurements to date.

Acknowledgements

We thank the staffs at Fermilab and collaborating institutions, and acknowledge support from the DOE and NSF (USA); CEA and CNRS/IN2P3 (France); FASI, Rosatom and RFBR (Russia); CAPES, CNPq, FAPERJ, FAPESP and FUNDUNESP (Brazil); DAE and DST (India); Colciencias (Colombia); CONACyT (Mexico); KRF and KOSEF (Korea); CONICET and UBACyT (Argentina); FOM (The Netherlands); PPARC (United Kingdom); MSMT (Czech Republic); CRC Program, CFI, NSERC and WestGrid Project (Canada); BMBF and DFG (Germany); SFI (Ireland); The Swedish Research Council (Sweden); Research Corporation; Alexander von Humboldt Foundation; and the Marie Curie Program.

References

- [1] J.C. Pati, A. Salam, Phys. Rev. D 10 (1974) 275;
E. Eichten, et al., Phys. Rev. D 34 (1986) 1547;
W. Buchmüller, D. Wyler, Phys. Lett. B 177 (1986) 377;
- E. Eichten, et al., Phys. Rev. Lett. 50 (1983) 811;
H. Georgi, S. Glashow, Phys. Rev. Lett. 32 (1974) 438.
- [2] M. Leurer, Phys. Rev. D 49 (1994) 333;
S. Davidson, D.C. Bailey, B.A. Campbell, Z. Phys. C 61 (1994) 613;
O. Shanker, Nucl. Phys. B 204 (1982) 375.
- [3] DØ Collaboration, B. Abbott, et al., Phys. Rev. Lett. 84 (2000) 2088.
- [4] CDF Collaboration, A. Abulencia, et al., hep-ex/0512055, Phys. Rev. D, submitted for publication.
- [5] DØ Collaboration, V.M. Abazov, et al., hep-ex/0511054, Nucl. Instrum. Methods Phys. Res. A, submitted for publication.
- [6] V.M. Abazov, et al., Nucl. Instrum. Methods A 552 (2005) 372.
- [7] G. Blazey, et al., in: U. Baur, R.K. Ellis, D. Zeppenfeld (Eds.), Proceedings of the Workshop QCD and Weak Boson Physics in Run II, Batavia, 2000, p. 47, hep-ex/0005012.
- [8] T. Sjöstrand, Comput. Phys. Commun. 82 (1994) 74.
- [9] R. Hamberg, W.L. van Neerven, T. Matsuura, Nucl. Phys. B 359 (1991) 343;
R. Hamberg, W.L. van Neerven, T. Matsuura, Nucl. Phys. B 644 (2002) 403, Erratum;
J. Pumplin, D.R. Stump, J. Huston, H.L. Lai, P. Nadolsky, W.K. Tung, JHEP 0207 (2002) 012, hep-ph/0201195.
- [10] M.L. Mangano, M. Moretti, F. Piccinini, R. Pittau, A. Polosa, JHEP 0307 (2003) 001.
- [11] CTEQ Collaboration, H.L. Lai, et al., Eur. Phys. J. C 12 (2000) 375.
- [12] R. Brun, F. Carminati, CERN Program Library Long Writeup W5013, 1993.
- [13] T. Junk, Nucl. Instrum. Methods Phys. Res. A 434 (1999) 435.
- [14] M. Krämer, T. Plehn, M. Spira, P.M. Zerwas, Phys. Rev. Lett. 79 (1997) 341.
- [15] J. Pumplin, D.R. Stump, J. Huston, H.L. Lai, P. Nadolsky, W.K. Tung, JHEP 0207 (2002) 012.